Manipulation Planning Using Wave Variables

Phongsaen Pitakwatchara and Jetnipit Arunrat

***Abstract*—There are plenty of low-level controllers for the robots to perform manipulation tasks. Most of them require specifying of either reference motion or force as the input. However, motion or force planning to interact with unstructured environment is very difficult. This letter proposes the use of wave variables which facilitate the computation of suitable reference motion or force through the *wave planner* framework. The notion is to specify the *supplied power*, via input wave, instead of desired *motion* or *force*. Input wave will be resolved into motion and force according to the port impedance. The method ensures safe manipulation when applying to passive control systems. Experimental results show advantages of using this wave planner with the impedance and force controllers.**

***Index Terms*—Manipulation planning, robot safety, wave variables, wave planning.**

I. Introduction

ROBOTS are getting closer to human as never before since they are becoming more autonomous and capable to perform complex tasks on their own thanks to recent leaps in artificial intelligence technology. It is projected that in the near future the robots will be able to naturally perform some mundane tasks such as cleaning or packing up things for us. However, most working robots today are built from metals or materials that are quite rigid. Hence there is an underlying problem of robot safety that needs to be solved before they can be deployed in daily environment.

Researchers have proposed new types of robots and actuators that are inherently safe. Meanwhile, there are efforts on designing the controllers that yields safe interaction with environment. Notably, impedance control was proposed [1] and is being used widely. The idea is to regulate the robot impedance, or admittance, appropriately for the task and environment involved. Hybrid force/motion control [2] is another approach to regulate the interaction force and admissible motion along the constrained and unconstrained directions respectively. Fundamentally, hybrid control requires perfect knowledge on the contact kinematic constraints while impedance control does not.

Manuscript received October 28, 2021; accepted March 11, 2022. Date of publication April 11, 2022; date of current version April 25, 2022. This letter was recommended for publication by Associate Editor Y. Sun and Editor H. Liu upon evaluation of the reviewers' comments. The work was supported in part by the Faculty of Engineering, Chulalongkorn University. *(Corresponding author: Phongsaen Pitakwatchara.)*

The authors are with the Department of Mechanical Engineering, Faculty of Engineering, Chulalongkorn University, Bangkok 10330, Thailand (e-mail: phongsaen.p@chula.ac.th; phongsaen@gmail.com).

This letter has supplementary downloadable material available at https://doi.org/10.1109/LRA.2022.3166442, provided by the authors.

Digital Object Identifier 10.1109/LRA.2022.3166442

Moreover, there are works on high-level planning which address safe manipulation issues. Artificial potential field [3] was used to attract the robot to the goal and repel it from the obstacles. Elastic strip framework [4] generated a task consistent real-time collision-free workspace volume from the planned motion. Optimization was used to generate the real-time adaptive motion planning [5] of redundant robots with moving obstacles. These planners assume no physical contact with the environment.

However, some robots interact closely with the environment and use force feedback in the planning stage as well. For instance, the robot would stop [6] or react properly [7] when collision was deduced. Constraints on joint torque limits were used in motion planning via incremental graph search algorithm [8]. A grasp planner that enables the robot to regrasp objects under changing external force was proposed [9]. In [10], actual motion was generated online from the trajectory-following and sensor-guided control such that the robot can react to unforeseen events instantaneously at any motion state.

Performing tasks in real world is daunting because we usually do not have precise model and enough information of the environment to perfectly plan the manipulation involving both force and motion. This is the case for hybrid control. In contrast, impedance control relieves the stringent planning by allowing the robot to tolerate with improper reference motion to a certain degree. It ensures acceptable interaction force response according to the specified robot impedance. However when interacting with rigid environment, large force could be developed easily even for small error in the planned motion. In this case, it is more natural to control the force which requires changing the structure of the controller. To meet the needs, good indicator to trigger the controller switching is necessary and the switching process must happen fast enough. Both are difficult to achieve in practice.

Contribution of this letter is a wave planner framework to determine reference motion or force for low-level robot controllers based on wave variables and environmental impedance. Some features and benefits are 1) It sets the *supplied power* used in performing the task. Thus, desired input force or motion and feedback values for determining input wave or supplied power need not be precise. Also, the amount of power drawn by the robot can be limited. 2) Reference motion or force for low-level controllers are resolved considering port impedance. Hence the manipulation and actual power consumed will comply with interacting environment. 3) Returning output wave contains information regarding interacting environment. Therefore, it may be helpful in identifying input wave, for instance, should it be computed from desired force or motion. Accordingly, the framework ensures safe manipulation when using with the

passive control system. Only passive system alone is not safe as shown by experiments in Section V.

Organization of the letter is as follow. Section II introduces wave variables and its characteristics. Wave planner framework consisting of designing suitable input wave and computing reference motion or force are presented in Section III and IV. Various experiments are presented in Section V, followed by some remarks and conclusions in Section VI.

II. Wave Variables

Wave variables are another representation of power variables (effort and flow) at a particular port. They comprise the input and output waves denoted as u and v. For the manipulation in $SE(3)$, the waves may be separated into linear (v) and angular (ω) vector components according to the following bijective transformation

$$\begin{aligned} u_v &\equiv \left\langle 1/\sqrt{2b_v} \right\rangle (b_v\dot{x} + f), \quad v_v \equiv \left\langle 1/\sqrt{2b_v} \right\rangle (b_v\dot{x} - f) \\ u_\omega &\equiv \left\langle 1/\sqrt{2b_\omega} \right\rangle (b_\omega\omega + \mu), \quad v_\omega \equiv \left\langle 1/\sqrt{2b_\omega} \right\rangle (b_\omega\omega - \mu) \end{aligned} \tag{1}$$

The effort (f, μ) denote force and couple vectors, while the flow $(\dot{x}, \omega)$ are for linear and angular velocity vectors at the port of interest. Adjustable parameters b_v and b_ω are the wave impedance that may be viewed as the weighting between effort and flow. The symbol $\langle\cdot\rangle$ denotes a 3×3 diagonal matrix of which its diagonal elements are the given argument. Equation (1) may be rewritten in different ways depending on the selected input and output variables. For instance,

$$V = 1/\sqrt{2b}(u + v), \quad F = \sqrt{b/2}(u - v) \tag{2}$$

is the inverse of (1) expressed using compact matrix-vector notations. Variable that is not v- or ω-subscript denotes the vector or matrix containing linear and angular components together, i.e. $V^\top = [\dot{x}^\top\ \omega^\top]$, $F^\top = [f^\top\ \mu^\top]$, $u^\top = [u_v^\top\ u_\omega^\top]$, $v^\top = [v_v^\top\ v_\omega^\top]$, $1/\sqrt{2b} = \text{diag}(\langle 1/\sqrt{2b_v}\rangle, \langle 1/\sqrt{2b_\omega}\rangle)$, and $\sqrt{b/2} = \text{diag}(\langle \sqrt{b_v/2}\rangle, \langle \sqrt{b_\omega/2}\rangle)$.

From (1) and (2), power flow into the port may be expressed in terms of wave variables as

$$P = F^\top V = (u^\top u - v^\top v)/2 \tag{3}$$

It is seen that wave variables are closely related to the power flow as their units are $[\sqrt{\text{Watt}}]$ and the input/output waves are associated with the power flow into/out of the port. Moreover, the transformation is lossless. Hence wave variables may be used to analyze passivity of the systems conveniently [11]. Unlike power variables, wave variables are robust to constant time delay in communication because the delayed power will just be temporarily stored. Therefore, communication through wave variables is also lossless. For this reason, they are widely applied to the teleoperation and distributed control systems [12], [13]. Commanding the wave variables are also flexible. For example, simple wave variable transmission scheme in [12] may be modified in order to guarantee passive teleoperation system for time-varying delayed communication [14].

Wave variables may be used to describe the manipulation as an alternative to power variables. If $v = u$ at the interaction port where the robot interacts with the environment, the robot undergoes steady motion in free space corresponding to $F = 0$ and V being some constant. Oppositely, $v = -u$ signifies the robot in static against some rigid constraint with $V = 0$ and F being constant. Hence, status of the manipulation may be deduced from the wave response.

Most environments are neither of these two extremes. Relationship between u and v described by the wave dynamics is thus more complicated. Still, simple enough dynamics may be derived and comprehend for ideal mass, spring, damper systems. This will be beneficial for designing input wave for the wave planner framework in Section III.

Wave dynamics of an unconstrained mass m may be derived as

$$\dot{v} + \lambda v = -\dot{u} + \lambda u \tag{4}$$

where $\lambda = b/m$. Applying a constant u to the system at rest, v evolves from $-u$ to u in the manner of the first order system response. The lighter the mass, the faster the response. At steady state, the mass will be traveling with constant speed $V = \sqrt{2/b}u$ and no power is consumed. If the mass encounters a rigid constraint, it will stop and instead apply constant force $F = \sqrt{2b}u$ to the constraint. Since $V = 0$, v reduces to $-u$.

On the other hand, wave dynamics of a spring with stiffness k having one end fixed may be derived as

$$\dot{v} + \lambda v = \dot{u} - \lambda u \tag{5}$$

with $\lambda = k/b$. Applying a constant u to the system at rest, v changes from u to $-u$. The stronger the spring, the faster the response. At steady state, the spring deforms to a certain distance with constant applied force $F = \sqrt{2b}u$ and no power is consumed. If the spring's fixed end is freed, the spring will travel with constant speed $V = \sqrt{2/b}u$ and apply no force. Since $F = 0$, v increases to u.

Wave dynamics of a damper with the damping constant c is simply

$$v = (1 - \lambda)/(1 + \lambda)u \tag{6}$$

where $\lambda = c/b$. v is merely the scaling of u. If $c \ll b$ or very light damper, it behaves close to free space and $v \approx u$. If $c < b$, the motion is subject to viscous friction and thus $0 < v < u$. If $c > b$, motion becomes more difficult like moving against the bumper and so $-u < v < 0$. If $c \gg b$ or very heavy damper, it acts like rigid constraint and thus $v \approx -u$. When $c = b$, $v = 0$ and the supplied power has all been used up. Other damping values dissipate less power.

Real environment may be viewed as a complex structure of connected masses, springs, and dampers. Response of each element thus affects the total wave response. Take the mass, spring, damper system in Fig. 1 as a simple example. After applying u_r, v_r is subject to the spring and damper dynamics initially but later influenced solely by motion of the mass. Response of v_e is similar to the output wave of pure mass except that its transient is as of the second order system due to interleaving parallel spring and damper.

Overall, wave variables unify force and motion indistinguishably as both are important for successful manipulation. They

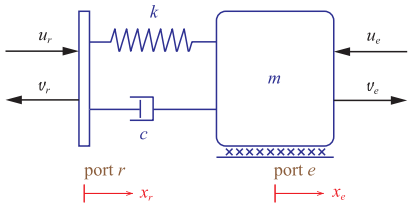

Fig. 1. Mass, spring, damper system.

provide insights about power flow in the system. Input wave encodes the power supplied to the port. Together with the output wave, actual power consumed is determined by (3). Key takeaways from wave dynamics analysis are $v = u$ for steady free motion with constant speed $V = \sqrt{2/b}u$, $v = -u$ for steady application of force $F = \sqrt{2b}u$ with no motion, and transient response is caused by the system dynamics. Heavy mass retards free motion, soft spring diminishes applied force, and damper hinders both pure motion and pure force.

III. Design of Input Wave

Figure 2 depicts the wave planner framework and its connection with other subsystems. We *command input wave* u_r, which implies setting up the *power* entering the robot. Then, depending on the type of robot controller, either motion V_r or force F_r is determined from u_r and its dual variable. The result serves as reference input to the controller. It complies with the environment in a sense that large motion and small force will be generated if the environment is compliant. On the other hand, it changes to small motion and large force automatically when the environment becomes stiff. This is in contrast with traditional robot control frameworks that either *motion* or *force* is commanded directly. It is very difficult to devise appropriate values in real-time for manipulation with unstructured environment, and also achieve it. Furthermore, actual power consumed to realize specified motion or force is not known beforehand and might be too much such that it harms the robot and environment.

It should be mentioned that the use of wave variables in this work is radically different from those in telerobotics. According to Fig. 3, here we design proper input wave using information such as desired motion or force, feedback signals, or triggering events in order to perform the task successfully. On the other hand, input and output waves are not by design in telerobotics application. They are determined straightforwardly from the definition of wave variables. Then, they are transmitted to the other side subject to time delay. Since the communication topology forms a delayed loop, *wave reflection* problem occurs that must be addressed [12]. However, wave variables in this work are not being used as the means for communication. Also, we have freedom to design the input wave. Therefore, we should not have to face with wave reflection in the wave planner framework.

Wave planner framework consists of designing appropriate input wave and computing reference value. In this section, we present 5 examples of determining input wave based on different requirements and variety of settings as follow.

A. Input Wave Based on Required Input Power

Basically, input wave may be determined from required input power P_d to drive the system and the action direction $\hat{e}_u$, i.e.

$$u_r = \sqrt{2P_d}\,\hat{e}_u \tag{7}$$

This is useful when the task description cannot be specified clearly in terms of motion or force. Note that actual power consumed is determined from (3), however.

B. Input Wave Based on Desired Motion or Force

For most tasks, desired motion or force, V_d or F_d, which can be visualized readily are roughly planned for unstructured environment. Input wave could then be assigned as

$$u_r = \sqrt{b/2}\,V_d \quad \text{or} \quad u_r = F_d/\sqrt{2b} \tag{8}$$

depending on the task performed. This is the value required to move in the free space with V_d, or to interact with the rigid constraint by F_d respectively. Note that both (7) and (8) restrict the amount of power consumed to a predetermined value. Utilizing these schemes with passive controllers, manipulation is thus inherently safe.

C. Input Wave to Achieve Desired Motion or Force

Nevertheless, V_d or F_d may not be achieved by (8) for the robot manipulation system due to its non-zero impedance and admittance. If impedance and admittance models $F_r = Z_r(V_r)$ and $V_r = A_r(F_r)$ at the controller input port are known, input wave

$$u_r = (bV_d + Z_r(V_d))/\sqrt{2b} \text{ or } u_r = (bA_r(F_d) + F_d)/\sqrt{2b} \tag{9}$$

yields desired values when enough power source is available.

Practical robot systems are far complicated to arrive at accurate model in real-time. Therefore, the notion of feedback will be employed in determining input wave. In particular,

$$u_r = (bV_d + F_r)/\sqrt{2b} \quad \text{or} \quad u_r = (bV_r + F_d)/\sqrt{2b} \tag{10}$$

where F_r and V_r are feedback reference force and motion at the controller input port. Effectively, portion of the input wave caused by associated force or motion to the desired motion or force has been compensated.

It should be pointed out that wave planning using (9) or (10) is proactive since it calls for sufficient power to secure V_d or F_d, which cannot be determined beforehand for unstructured system. The power might be too large for safety manipulation. As shown in Section IV-A, this is indeed equivalent to the usual practice of assigning V_d or F_d to the controller directly. To make the manipulation safe, (9) or (10) should be bounded by some power limit.

It is observed from wave dynamics in Section II that u_r and v_r are of the same sign if the system is moving using only small force. Since it can move nearly freely, motion should be commanded. On the other hand, when the system undergoes motion with large force, the signs will be different. In this case, we should attempt to regulate the force. Hence, the sign of v_r

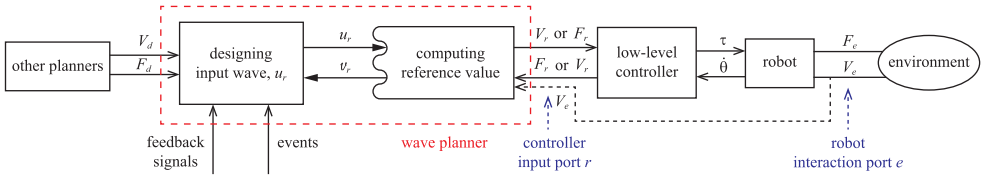

Fig. 2. Wave planner framework.

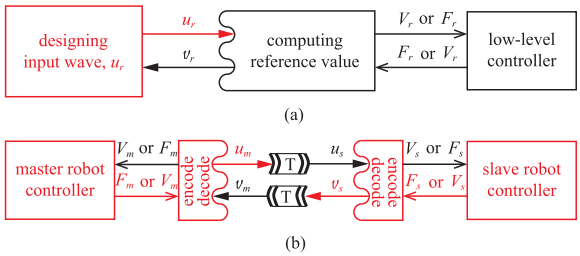

Fig. 3. (a) wave planner and (b) wave telerobotic frameworks. Origin of input waves are shown in red color.

may be used as the indicator to switch between two modes for computing input wave of (8)–(10) from either V_d or F_d. At the moment of mode switching, V_d and F_d should be such that $F_d = bV_d$ in order to make the supplied power smooth.

D. Input Wave Influenced by External Events

Additionally, information such as vision or sound at different ports might play a part in determining input wave. For example, an unexpected wave surge at the robot interaction port u_e could signal the manipulation is experiencing unforeseen circumstances such as crashing into the rigid constraint or slipping out suddenly when the harness is removed. Thus, u_r should be reduced from the designed value u_{r0} as

$$u_r = u_{r0} - \mathrm{sgn}(u_{r0}) K \|\dot{u}_e\| \hat{e}_{u_{r0}}, \quad K > 0 \tag{11}$$

Hence, it is quite flexible for robot to perform the manipulation by planning input wave in response to external events since *supplied input power* and *action direction* are the only two quantities needed to command properly.

E. Input Waves for Cooperative Fingers

Wave planner may be readily applied to cooperative manipulation planning as well. Take an example of moving an object with a simple gripper having 2 fingers controlled separately. See Fig. 4. If the object is to be moved with desired velocity $\dot{x}_d$ and gripping force f_d, left (le) and right (ri) fingers should supply input waves u_{le} and u_{ri} to the object as

$$u_{\mathrm{le}} = (b\dot{x}_d + f_d)/\sqrt{2b} \qquad u_{\mathrm{ri}} = (b\dot{x}_d - f_d)/\sqrt{2b} \tag{12}$$

As explained in Section IV-A, (12) could be used as input waves to the left and right fingers if their dynamics are good enough.

IV. Computing Reference Motion or Force

After the input wave is determined, reference motion or force may be computed depending on the type of robot controller used. Impedance controller shapes the impedance dynamics at the robot interaction port. Refer to Fig. 1. If desired stiffness K and damping C at the end effector are specified while the mass is unchanged, passive task-space impedance control law expressed in the body frame $\{b\}$ will be

$${}^bF_r = \begin{bmatrix} C_v({}^b\dot{x}_r - {}^b\dot{x}_e) + K_v R_b^\top (x_r - x_e) \\ C_\omega({}^b\omega_r - {}^b\omega_e) + \frac{1}{2}K_\omega({}^bR_{br} - {}^bR_{br}^\top)^\vee \end{bmatrix} \tag{13}$$

where $\{br\}$ is the reference pose frame and $(\cdot)^\vee$ transforms a skew-symmetric matrix to its vector representation.

Since the controller accepts reference motion as input, it and output wave may be computed using (1) as

$$\begin{aligned} {}^bV_r &= \sqrt{2/b}\,[{}^bR_{br}]\,{}^{br}u_r - {}^bF_r/b \\ [{}^bR_{br}]\,{}^{br}v_r &= [{}^bR_{br}]\,{}^{br}u_r - \sqrt{2/b}\,{}^bF_r \end{aligned} \tag{14}$$

Note that (14) is expressed in $\{b\}$ and $[{}^bR_{br}]$ denotes the 6×6 block-diagonal matrix $\mathrm{diag}({}^bR_{br}, {}^bR_{br})$ for clarity. ${}^bF_r$ may be sensed directly or computed from the control law. Applying (13) to (14), ${}^bV_r$ and ${}^{br}v_r$ may be resolved in terms of ${}^{br}u_r$ and ${}^bV_e$.

Force controller controls robot interaction force to follow the reference value. A number of force control laws have been proposed. Regardless of any controller used, its reference force and output wave may be determined from (1) as

$$F_r = \sqrt{2b}\,u_r - bV_r \qquad v_r = -u_r + \sqrt{2b}\,V_r \tag{15}$$

Robot motion V_e may be feedback and used for V_r in (15). This is technically incorrect because the wave planner is applied to the force controller input port, which indeed has no reference motion associated; it is merely the signal, not power, port. Nevertheless, if the force controller performs well, V_e may be feedback and used as the substitute for V_r. The result approximates as if the wave planner is applied at the interaction port directly. Overall, wave planner facilitates power flow analysis in robot manipulation. It generates compliant reference motion or force to the controller from desired motion or force and actual motion feedback. The proposed framework is adaptable and versatile enough to use in conjunction with several low-level controller architectures.

A. How Does the Wave Planner Work?

In the following, we analyze the wave planner for some input wave u_r proposed earlier to understand how does it work. If u_r in Section III-B is used, reference motion (14) or

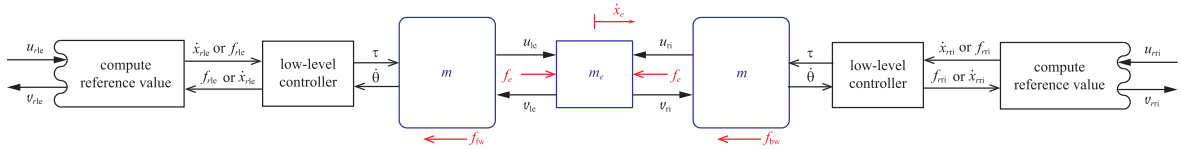

Fig. 4. Input waves for the gripper to move the object with desired velocity $\dot{x}_d$ and gripping force F_d.

force (15) becomes

$$V_r = V_d - Z_r(V_r)/b \quad \text{or} \quad V_r = F_d/b - Z_r(V_r)/b$$
$$F_r = F_d - bA_r(F_r) \quad \text{or} \quad F_r = bV_d - bA_r(F_r) \tag{16}$$

This implies motion or force planning will take port and wave impedance into consideration. Reference values will be reduced from the desired ones by the impedance. Wave impedance b acts as a threshold judging the relative size of Z_r. It can be adjusted on the fly according to the task situation. If Z_r is small, F_d will be reduced significantly while V_d is not affected much. It agrees with light and soft systems that requires just a small amount of force to maneuver. Large motion is acceptable and associated force is still small. On the contrary, V_d will be largely reduced while F_d is not much for high Z_r. Heavy and stiff systems can withstand large force. However, constraint violation by large motion should not be allowed.

It is seen that wave planner automatically generates reference controller input value appropriately according to the impedance as well as the desired value. Consequently, if it is certain that finally the robot will be moving the object around, we could specify $u_r = \sqrt{b/2}\, V_d$ throughout the course safely without switching the mode. As the movement gets ease, V_r will be increased toward V_d. Similarly, if finally the robot will be applying force to the constraint, $u_r = F_d/\sqrt{2b}$ will provide small F_r during approaching the constraint. Once reached, F_r will be increased to F_d.

When u_r in Section III-C is used, V_r or F_r would become simply

$$V_r = V_d \qquad F_r = F_d \tag{17}$$

Implicitly, impedance is not utilized to correct the planning. The result should not be surprised because port model or feedback signal is employed in generating input wave to achieve the desired values, which have been verified here.

If u_r of Section III-E is applied to the 2-fingered gripper diagrammed in Fig. 4 for grasping and moving the object, reference motion or force (magnitude) for the left and right fingers will be

$$\dot{x}_{r\text{le}} = \dot{x}_d + f_d/b - f_{r\text{le}}/b \quad \dot{x}_{r\text{ri}} = \dot{x}_d - f_d/b + f_{r\text{ri}}/b$$
$$f_{r\text{le}} = f_d + b\dot{x}_d - b\dot{x}_{r\text{le}} \qquad f_{r\text{ri}} = f_d - b\dot{x}_d + b\dot{x}_{r\text{ri}} \tag{18}$$

Reference motion is used with impedance controller. When the object movement is stabilized, both fingers and the object will be moving altogether with same constant velocity that is also the common reference velocity $\dot{x}_r$. Thus, addition of $\dot{x}_{r\text{le}}$ and $\dot{x}_{r\text{ri}}$ in (18) would be

$$2\dot{x}_r = 2\dot{x}_d + (f_{r\text{ri}} - f_{r\text{le}})/b \tag{19}$$

If $f_{r\text{ri}} = f_{r\text{le}} = f_r$, $\dot{x}_r = \dot{x}_e = \dot{x}_d$. Substituting this result back into (18), it is seen that $f_r = f_d$ too. This situation happens when friction of the gripper is negligible. Dynamic equilibrium of each finger reveals that gripping force $f_e = f_d$ is achieved.

However, it is common that $f_{r\text{ri}} \neq f_{r\text{le}}$ due to friction. In this case, dynamic equilibrium when the gripper and object move to the right requires $f_{r\text{le}} - f_{r\text{ri}} = 2f$ where $2f = f_{\text{fw}} + f_{\text{bw}}$ is the total friction caused by forward and backward friction of each finger driving system. Applying this to (19), $\dot{x}_r = \dot{x}_e = \dot{x}_d - f/b$. It is apparent that the object will be moving slower than desired. Substituting the result into (18), $f_{r\text{le}} = f_d + f$ and $f_{r\text{ri}} = f_d - f$. From dynamic equilibrium of the finger, $f_e = f_d + (f_{\text{bw}} - f_{\text{fw}})/2$.

Reference force in (18) may be applied to the force controller. If the object movement is stabilized already, addition of $f_{r\text{le}}$ and $f_{r\text{ri}}$ yields

$$f_{r\text{le}} + f_{r\text{ri}} = 2f_d \tag{20}$$

If the controller functions well, f_e will catch up with f_r quickly. Using the fact that $f_{e\text{le}} = f_{e\text{ri}}$, (20) shows that $f_r = f_e = f_d$. Substituting the result into (18), $\dot{x}_r = \dot{x}_e = \dot{x}_d$ regardless of friction. Therefore, the gripper may use (12) to move the object with $\dot{x}_d$ and f_d readily. However, friction will slow down $\dot{x}_e$ and make f_e differ from f_d if it is used with the impedance controller. On the other hand, the gripper can move the object efficiently using non-passive force controller since the friction has been compensated.

Overall, main takeaway from this section is it is easier and more intuitive to plan the input wave than motion or force directly. This is because the information used to determine input wave need not be precise. Remember planning the wave is essentially equivalent to setting up the supplied power for performing the task. Another reason owes to consideration of port impedance when resolving reference motion or force that is compliant to the environment.

V. Experiments

We have performed various experiments to illustrate improved behaviors of the robot during manipulation with unstructured environments using the wave planner against some ad hoc planning. Accompanied videos are available in the multimedia attachment.

A. Touching the Wall

A robot is controlled to touch a rigid wall with desired approaching velocity $\dot{x}_d = 80\,\text{mm/s}$ and desired contact force $f_d = 40\,\text{N}$. Location of the wall is not known. For the

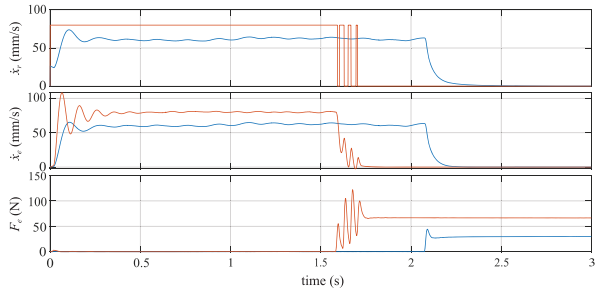

Fig. 5. Reference velocity, robot velocity, and contact force of the robot touching the rigid wall. Impedance controller (21) is used with reference motion determined from (14) (blue) and (22) (red).

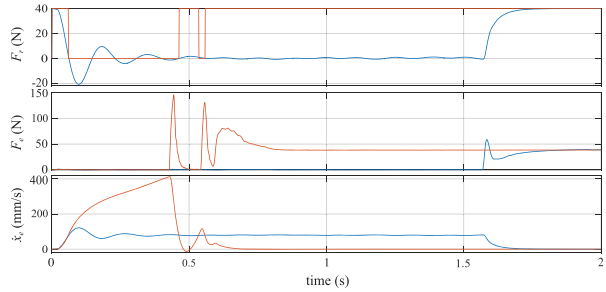

Fig. 6. Reference force, contact force, and robot velocity during touching the rigid wall. Force controller (23) is used with reference force determined from (15) (blue) and (24) (red).

impedance-controlled robot, a simple impedance control law

$$f_r = c_d(\dot{x}_r - \dot{x}_e) + k_d(x_r - x_e) \tag{21}$$

is used to control the robot with $k_d = 10\,\mathrm{kN/m}$ and $c_d = 1\,\mathrm{kN{\cdot}s/m}$. Besides suitable impedance parameters, good reference motion $\dot{x}_r$ is needed to perform the task successfully. We employ wave planner with a simple fixed input wave $u_r = \sqrt{b/2}\dot{x}_d$ and $b = 500\,\mathrm{N{\cdot}s/m}$ to compute $\dot{x}_r$ according to $\dot{x}_r = \sqrt{2/b}u_r - f_r/b$, which is a scalar version of (14). For comparison, we manually design $\dot{x}_r$ based on actual contact force f_e as

$$\dot{x}_r = \begin{cases} \dot{x}_d, & f_e < f_d \\ 0, & f_e \geq f_d \end{cases} \tag{22}$$

Graph of $\dot{x}_r$, $\dot{x}_e$, and f_e are plotted in Fig. 5 for both cases. It is seen that $\dot{x}_r$ of the wave planner jumps from 0 to some positive value due to low impedance at the beginning. Then, complex robot friction starts to impede $\dot{x}_r$. Eventually, f_r strives to balance with the changing friction making $\dot{x}_r$ and $\dot{x}_e$ stay below $\dot{x}_d$ and oscillate around $60\,\mathrm{mm/s}$. Due to a fixed amount of supplied power by a predetermined constant of u_r, $\dot{x}_r = \dot{x}_d$ cannot be ensured. If b is increased or the friction reduced, $\dot{x}_r$ will be closer to $\dot{x}_d$ during approaching the wall. When the robot touches the wall, high impedance causes $\dot{x}_r$ to reduce to 0 while f_e overshoots to f_d and drops down to $30\,\mathrm{N}$ at steady state because approximately $10\,\mathrm{N}$ of $f_r = f_d$ is absorbed into static friction.

If (22) is used, $\dot{x}_e$ overshoots and oscillates during transient due to step change of $\dot{x}_r$. Although impedance controller is used, the control system draws exhaustive power such that $\dot{x}_e$ ripples around $\dot{x}_d$ at steady state motion regardless of the robot and environment impedance. Thus, the robot spends less time to reach the wall. As it touches the wall, f_e exceeds f_d which makes $\dot{x}_r$ become 0. In turn, $\dot{x}_e$ and f_r are reduced. Hence f_e drops below f_d and $\dot{x}_r$ rises up to $\dot{x}_d$ again. This intermittent pushing lasts for a few cycles before settling with some $f_e > f_d$ at which $\dot{x}_r = \dot{x}_e = 0$. Power consumed when the wave planner is used with impedance controller does not exceed $\frac{1}{2}u_r^2 = 0.8\,\mathrm{W}$ and total energy used is $1.25\,\mathrm{W{\cdot}s}$. When (22) is used instead, power cannot be controlled. Its maximum reaches $10.56\,\mathrm{W}$ during wall collision and total energy increased to $1.75\,\mathrm{W{\cdot}s}$. Therefore, using the wave planner to plan reference motion for the robot impedance controller is intuitive and results in passive and more stable interaction with unplanned rigid environment.

For the force-controlled robot, a Proportional-Integral (PI) force controller

$$f = f_r + k_p(f_r - f_e) + k_i\int(f_r - f_e)d\tau \tag{23}$$

is used to perform the same task. Its control gain are $k_p = 0.01$ and $k_i = 0.01$. The controller requires good reference force f_r to perform the task. We use wave planner with a simple fixed input wave $u_r = f_d/\sqrt{2b}$ and $b = 500\,\mathrm{N{\cdot}s/m}$ to compute f_r according to (15). For comparison, we manually assign f_r based on the robot velocity $\dot{x}_e$ as

$$f_r = \begin{cases} f_d, & \dot{x}_e \leq \dot{x}_d \\ 0, & \dot{x}_e > \dot{x}_d \end{cases} \tag{24}$$

Figure 6 shows the plot of f_r, f_e, and $\dot{x}_e$. When (15) is used, initially $f_r = f_d$ ramps f up by the integral term in (23). Excessive force f makes $\dot{x}_e$ overshoot. In turn, it lowers $f_r < 0$ and thus f is reduced. Together with large developing friction, $\dot{x}_e$ decreases, by which f_r will now increase. These cyclic responses may be suppressed using smaller k_i. Continuing with $f_e = 0$, eventually only the integral term will be balanced with the robot friction. As a result, f_r stays close to 0 and hence $\dot{x}_e$ be close to $\dot{x}_d$. Small fluctuation is due to friction force variation. When the robot touches the wall, reduced $\dot{x}_e$ causes f_r to increase to f_d. The integral error then increases f rapidly, such that f_e overshoots and then undershoots to cancel with the negative integral. Finally, steady state value of the integral is absorbed into static friction and therefore $f_e = f_r = f_d$. Force controller does not consume power more than $\frac{1}{2}u_r^2 = 0.8\,\mathrm{W}$ at any moment. Yet, it periodically returns the power up to $2.52\,\mathrm{W}$ back in order to slow down the exceeding speed.

If (24) is used instead, a pulse of $f_r = f_d$ is applied whenever $\dot{x}_e$ is below $\dot{x}_d$. Effectively, the integral term in (23) is building up large f that results in very large $\dot{x}_e$. The robot hits the wall at high speed, where actual power consumed reaches the peak of $9.47\,\mathrm{W}$, and large impact force f_e is generated. It reduces the integral term and f abruptly. Together with f_e, $\dot{x}_e$ decreases to the point that it becomes negative. The robot bounces back. At the same time, a new pulse of $f_r = f_d$ makes the robot hit the wall again. Finally, large and sluggish overshoot of f_e reduces

f such that, at steady state, it balances with $f_e = f_d$ and the static friction. Total energy used is $2.92\,\mathrm{W{\cdot}s}$. Apparently, using the wave planner to plan reference force for the robot force controller is intuitive and yields stable interaction and desired force with unplanned rigid environment.

B. Pick and Place the Object

Pick and place the object is a common yet nontrivial task for unplanned environment where information about the object such as its location, shape, or hardness are not known precisely. It is shown that we can apply wave planner in conjunction with either impedance or force controller to command the gripper to pick and place an object readily.

A simple 1-DOF rigid gripper having 2 fingers controlled separately is used to pick up a 338.65 gram finished steel plate placed at some unknown location within the gripper stroke. The task is to grip the plate and move it to the right by 40 mm. Suitable gripping force f_d of $40\,\mathrm{N}$ is required to grasp the plate firmly during task execution.

For clarity, we concentrate on collaborative manipulation along the gripping direction only. The task may be decomposed into 3 phases, i.e. grasping, moving to a new place, and releasing the object. In phase 1, f_d should be applied in order to grasp the object firmly. Thus, we may command the left and right finger input waves as

$$u_{r\mathrm{le}} = f_d/\sqrt{2b} \qquad u_{r\mathrm{ri}} = -f_d/\sqrt{2b} \tag{25}$$

Next, input waves are commanded based on (12) in phase 2 where the same f_d is retained. However, desired velocity $\dot{x}_d$ must be assigned properly, upon which updated distance to the goal location, $x_g - x_e$, may be conditioned. Specifically,

$$u_{r\mathrm{le}}, u_{r\mathrm{ri}} = \begin{cases} \sqrt{b/2}\,\dot{x}_{d1} \pm f_d/\sqrt{2b}, & x_g - x_e > g_1 \\ \sqrt{b/2}\,\dot{x}_{d2} \pm f_d/\sqrt{2b}, & g_2 < x_g - x_e \le g_1 \\ \frac{x_g - x_e}{g_2}\sqrt{b/2}\,\dot{x}_{d2} \pm f_d/\sqrt{2b}, & x_g - x_e \le g_2 \end{cases} \tag{26}$$

are the left (using $+f_d$) and right (using $-f_d$) finger input waves that move the object rightward to the goal position $x_g = 40\,\mathrm{mm}$ with respect to the gripping location. In the beginning where the object is far from the goal than $g_1 = 35\,\mathrm{mm}$, $\dot{x}_d = \dot{x}_{d1} = 30\,\mathrm{mm/s}$. When the object moves past g_1 but still far from the goal than $g_2 = 5\,\mathrm{mm}$, $\dot{x}_d = \dot{x}_{d2} = 40\,\mathrm{mm/s}$. Finally, when the distance to the goal is less than g_2, $\dot{x}_d$ is reduced to 0 proportionally. Once it is at x_g, phase 3 is entered. The object may be released by gradually reducing the input wave to 0 and extending to some negative value. Consequently, f_e will be decreasing to 0 gently while the gripper starts to open.

Figure 7 depicts $\dot{x}_r$ vs. $\dot{x}_e$ and f_r vs. f_e of both fingers when impedance controller (21) with $k_d = 10\,\mathrm{kN/m}$, $c_d = 1\,\mathrm{kN{\cdot}s/m}$, and input waves (25)–(26) with $b = 1\,\mathrm{kN{\cdot}s/m}$ are used. Initially, the fingers move toward the rigid plate with $\dot{x}_e$ track $\dot{x}_r$ closely below f_d/b and fluctuate around $30\,\mathrm{mm/s}$ due to varying friction that balance with f_r. Then, grasping is performed smoothly even though the gripper and the plate are rigid. Stable $f_e = 30\,\mathrm{N} < f_d$ due to static friction.

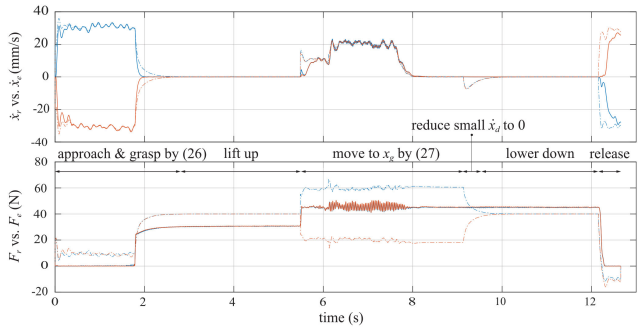

Fig. 7. Reference (dashed line) vs. actual (solid line) velocity, and reference (dashed line) vs. gripping (solid line) force of the left (blue) and right (red) fingers picking up the object using wave planner and impedance controller.

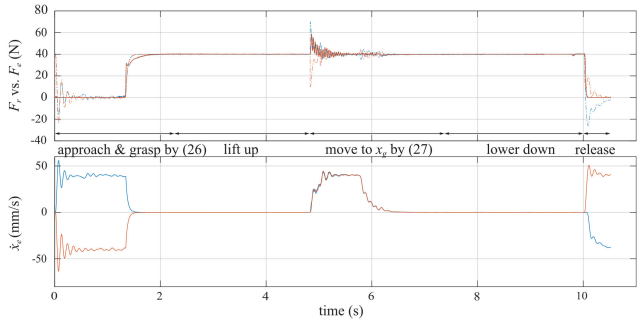

Fig. 8. Reference (dashed line) vs. gripping (solid line) force, and velocity of the left (blue) and right (red) fingers picking up the object using wave planner and force controller.

Next, the object is lifted up to a certain height and moved to x_g using (26). Referring to Section IV-A, $\dot{x}_r < \dot{x}_d$ and f_r bifurcates for the left and right finger due to friction. During dynamic equilibrium motion, $\dot{x}_e$ tracks $\dot{x}_r$ while f_e increases and fluctuates around $46\,\mathrm{N}$. Dynamic friction f_{fw} and f_{bw} are identified from the data as 14 and $26\,\mathrm{N}$ respectively.

Friction makes the gripper stop at $x_e = 37.4\,\mathrm{mm}$ before reaching x_g. This is due to reduction of $\dot{x}_d$ to a low enough value, when $x_g - x_e \le g_2$, such that $\dot{x}_r = 0$. It may also be understood that reducing $\dot{x}_d$ brings the supplied power of the left and right fingers closer to each other such that at some point the net power is not enough to overcome the friction anymore. We solve the problem by reducing $\dot{x}_d$ to 0 gradually. From (18), $\dot{x}_r < 0$ and x_r is reduced. In turn, f_r decreases and increases for the left and right fingers to f_d. Eventually, $\dot{x}_r = 0$ again. Meanwhile, change of f_r makes the friction of each finger driving system transition from dynamic to static one. Hence the gripper still does not move and constant f_e is retained. Finally, the object is lowered down and u_r slowly reduced to negative value. f_e reduces and the gripper opens to release the object.

Input waves (25)–(26) are also applied to the force controller (23) using $k_p = 0.01$ and $k_i = 0.005$. Figure 8 shows the result. Overall, $\dot{x}_d$ and f_d are achieved thanks to active force controller that infuses additional power to compensate for the friction. The object has reached x_g, at which $\dot{x}_d$ is reduced to 0 as planned. However, overshoots at the beginning of the gripper motion in phase 1 and 2 are largely due to abrupt step change of

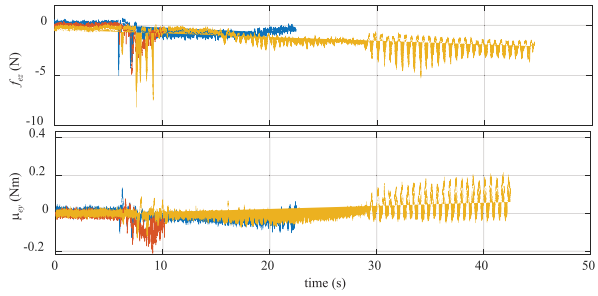

Fig. 9. Reaction force and couple for peg-in-hole using impedance controller and wave planner with small wave impedance (blue), large wave impedance with corrected input wave (red), and no wave planner (yellow).

input wave. Subsequent oscillation comes from force controller dynamics and friction variation.

C. Peg in Hole

We apply the wave planner for motion planning of a UR5e robot arm of Universal Robots to perform the classic peg-in-hole problem. A peg of $\phi 10\,\mathrm{mm}$ and $50\,\mathrm{mm}$-long is to be inserted into a hole of $\phi 10.5\,\mathrm{mm}$ and $40\,\mathrm{mm}$-deep while maintaining the interaction force below $10\,\mathrm{N}$ throughout. Both are made of Aluminium alloy 6061-T6. The hole is tilted from the vertical by 5°. The peg is initially placed at $100\,\mathrm{mm}$ above and $\pm 1\,\mathrm{mm}$ off-centered with the hole entrance. These geometrical knowledge is not exploited in manipulation. Hence, the experiment will be engaged with rich interaction between them in full dimensions.

Tool frame $\{b\}$ is attached at the tool tip. It has the z-axis aligning with and pointing outward the peg, and the y-axis pointing into the robot tool I/O connector. Initially, it is aligned with the reference tool frame $\{br\}$. Impedance controller (13) is used to control robot motion with $K_v = 500\,\mathrm{N/m}$, $C_v = 100\,\mathrm{N{\cdot}s/m}$, $K_\omega = 50\,\mathrm{Nm/rad}$, and $C_\omega = 10\,\mathrm{Nm{\cdot}s/rad}$ in all directions. The robot assumes the peg and hole are in-line vertically. According to natural constraint of the insertion task, it is suggested that in $\{br\}$ $f_{dx} = 0$, $f_{dy} = 0$, $\mu_{dx} = 0$, $\mu_{dy} = 0$, $\omega_{dz} = 0$, and $\dot{x}_{dz} = 10\,\mathrm{mm/s}$ chosen as desired velocity. From these values, corresponding input waves are designed using (8). When the peg is far from the hole, $b_v = 5000\,\mathrm{N{\cdot}s/m}$ and $b_\omega = 500\,\mathrm{Nm{\cdot}s/rad}$ are used. However, the values reduces to 100 and 10, respectively, when the peg is close to the hole entrance such that the manipulation becomes more sensitive to rigid environment, as mentioned in Section IV-A.

Another experiment is performed by modifying input wave based on the change of reaction wave at the tool tip as in (11) while retaining large wave impedance. For comparison, task execution using pure impedance controller is also conducted. However, $\dot{x}_{dz} = 1\,\mathrm{mm/s}$ is used, which is 10 times slower, otherwise the reaction force will exceed $10\,\mathrm{N}$. Reaction force f_{ez} and couple μ_{ey} at the tool tip are plotted in Fig. 9. The experiments show the readiness of wave impedance in altering manipulation behavior and how feedback information can be helpful in planning the right input wave. Using reaction wave to reorient the peg correctly, time to complete the task is reduced from 22.5 to 10.2 seconds. Pure impedance controller suffering from small reference force consumes the longest time period. All experimental results show that robot manipulation can be accomplished readily and intuitively using wave planner with existing standard controllers. This new manipulation planner promotes the robots to perform challenging tasks in real world safely.

VI. Conclusion

Wave planner framework has been proposed to command the robot manipulation in unstructured environment where force or motion is not obvious or difficult to plan. By this means, input wave related to supplied power for the tasks may be determined from desired motion, force, or other requirements, as well as available feedback information. We have presented several designs of input wave. They are flexible and intuitive. Input wave will then be resolved into reference force and motion according to the port impedance. It is shown that input wave provides desired motion when the impedance is small. On the other hand, desired force is generated with large environmental impedance. As a result, computed reference value for the underlying low-level controller complies with the environment the robot is interacting. Moreover, maximum power consumed can be limited by the input wave. Therefore, safe manipulation which is an important key for the robot to perform the tasks successfully may be achieved. Ongoing work of creating an intelligent agent that learns the wave planner for a variety of tasks is under investigation. The robot should be able to perform a choir of tasks autonomously in real world setting.

References

[1] N. Hogan, "Impedance control: An approach to manipulation," *ASME J. Dyn. Syst., Meas., Control*, vol. 107, no. 1, pp. 1–24, 1985.
[2] V. Ortenzi, R. Stolkin, J. Kuo, and M. Mistry, "Hybrid motion/force control: A review," *Adv. Robot.*, vol. 31, no. 19/20, pp. 1102–1113, 2017.
[3] O. Khatib, "Real-time obstacle avoidance for manipulators and mobile robots," *Int. J. Robot. Res.*, vol. 5, no. 1, pp. 90–98, 1986.
[4] O. Brock and O. Khatib, "Elastic strips: A framework for motion generation in human environments," *Int. J. Robot. Res.*, vol. 21, no. 12, pp. 1031–1052, 2002.
[5] J. Vannoy and J. Xiao, "Real-time adaptive motion planning (RAMP) of mobile manipulators in dynamic environments with unforeseen changes," *IEEE Trans. Robot.*, vol. 24, no. 5, pp. 1199–1212, Oct. 2008.
[6] S. Morinaga and K. Kosuge, "Collision detection system for manipulator based on adaptive impedance control law," in *Proc. Int. Conf. Robot. Autom.*, 2003, pp. 1080–1085.
[7] S. Haddadin, A. A. -Schaffer, A. De Luca, and G. Hirzinger, "Collision detection and reaction: A contribution to safe physical human-robot interaction," in *Proc. Int. Conf. Intell. Robots Syst.*, 2008, pp. 3356–3363.
[8] R. Holladay, T. L. -Perez, and A. Rodriguez, "Force and motion constrained planning for tool use," *Proc. Int. Conf. Intell. Robots Syst.*, 2019, pp. 7409–7416.
[9] L. Chen, L. F. C. Figueredo, and M. R. Dogar, "Manipulation planning under changing external forces," *Auton. Robots*, vol. 44, pp. 1249–1269, 2020.
[10] T. Kroger and F. M. Wahl, "Online trajectory generation: Basic concepts for instantaneous reactions to unforeseen events," *IEEE Trans. Robot.*, vol. 26, no. 1, pp. 94–111, Feb. 2010.
[11] M. R. Wohlers, *Lumped and Distributed Passive Networks*. New York, NY, USA: Academic Press, 1969.
[12] G. Niemeyer and J. J. Slotine, "Telemanipulation with time delays," *Int. J. Robot. Res.*, vol. 23, no. 9, pp. 873–890, 2004.
[13] C. Ott and Y. Nakamura, "Employing wave variables for coordinated control of robots with distributed control architecture," in *Proc. Int. Conf. Robot. Autom.*, 2008, pp. 575–582.
[14] P. Pitakwatchara, "Wave correction scheme for task space control of time-varying delayed teleoperation systems," *IEEE Trans. Control Syst. Technol.*, vol. 26, no. 6, pp. 2223–2231, Nov. 2018.